Study of Analysis Method for Conducted Noise Caused by High Frequency Leakage Current for Servo Drive Systems

HAMANA Kentaro, TOKUSAKI Hiroyuki and UEMATSU Takeshi

The declining working population and the energy saving of production sites for decarbonization have become major social issues. Toward this end, methods to effectively utilize the regenerative power of motors have been proposed, and DC powering of servo drives is expected to achieve this. On the other hand, compared to the current mainstream AC-powered systems, DC-powered servo drive systems tend to cause noise generated by one servo drive to be circulated to other servo drives, which raises concerns about malfunctioning problems. In particular, conducted noise caused by high-frequency leakage current from the shielded cable between the servo drive and the motor is a problem. Since this conducted noise is a factor that prolongs the product development period of servo drives, an analysis method that can study solutions upstream of the development process is needed.

In this paper, we investigate a conducted noise analysis method that can evaluate the effects of high-frequency leakage current from shielded cables on the power system and other equipment in an AC power supply system with a view to future DC power supply systems in order to shorten the development period of servo drives. Using this method, the phenomenon of conducted noise was reproduced for a servo drive system when the cable length and number of axes of the shielded cable were changed.

1. Introduction

In recent years, the introduction of robots to production sites is required because of the declining working population. Generally, the robots employ servo drives and electric motors with synchronization and high-speed, high precision control of several to several dozen axes. On the other hand, saving energy at production sites has become a major social issue from the social request for decarbonization. It is estimated that annual power consumption by industrial motors occupies about 75% of that in industrial sectors[1], and the method for effectively utilizing the regenerative power of motors is proposed to realize energy savings[2].

As one of its specific methods, DC powering of servo drives for which AC powering is currently the mainstream is studied[3]. Fig. 1 shows configurations of an AC-powered servo drive system and a DC-powered system.

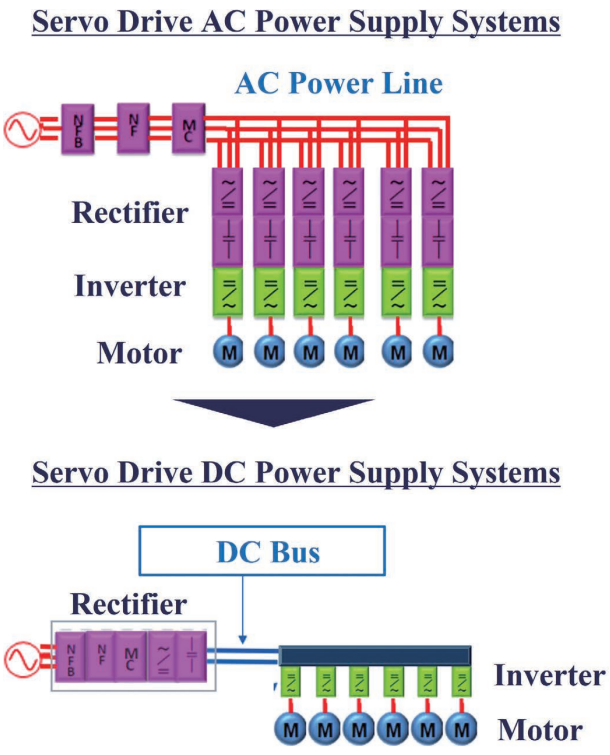

Fig. 1 AC-powered servo drive system and DC-powered system

Contact : *HAMANA Kentaro* kentaro.hamana@omron.com

The AC power supply system has a configuration where the rectifier and inverter circuits are loaded onto a servo drive, and a motor is connected to a servo drive. The multiaxial servo drive with several to several dozen axes and the motor are connected to the AC power line in parallel. On the other hand, the DC power supply system has a configuration where the rectifier circuits are consolidated into one circuit. The multiaxial inverter circuit and motor are connected in parallel to the DC bus after AC/DC conversion by the rectifier circuit.

The DC power supply system can be miniaturized, in addition to the effective utilization of regenerative power, and therefore have a configuration advantageous for the increase in the number of axes. On the other hand, since an inverter circuit is connected to the DC bus in parallel without passing through the rectifier circuit, the electromagnetic noise generated on the inverter circuit goes round into the other inverter circuit more easily than the AC power supply system. Since this noise suppression is a factor that prolongs the product development period, an analysis method that can be verified upstream of the development process is needed. Specifically, we can utilize the analysis to study the noise filter configuration and the suppression for resonance.

Circuit configuration elements of servo drives for the AC power supply system and the DC power supply system are common, and the analysis technique built for the AC power supply system can be deployed to the DC power supply system. Therefore, in this paper, the AC power supply system is taken as the object of study as the previous step of study of the DC power supply system.

The PWM inverter using a power semiconductor device is adopted for the inverter circuit of the servo drive in order to control the position, speed, and torque of the motor with high speed and high accuracy. In recent years, the next generation power semiconductors, such as silicon carbide (SiC) and gallium nitride (GaN), have been promoted for power semiconductor devices, and the carrier frequency of the PWM inverter is becoming higher. An issue of electromagnetic noise due to the increase of high-frequency leakage current flowing to the ground line (GND) through stray capacitance of the cable and motor between the servo drive and the motor is pointed out as associated with this higher frequency[4]. Regarding high-frequency leakage current flowing to the grounding wire through stray capacitance of the motor winding by switching of the PWM inverter, quantitative theoretical studies were so far performed, and an equivalent circuit model is shown[4]. One of phenomena of electromagnetic noise generated by this high-frequency leakage current is conducted emission. A technique for quantitatively estimating the conducted emission generated by the PWM inverter by simulation is proposed[5,6].

It is shown that the main factor in this conducted emission is common mode noise by the leakage current flowing through the stray capacitance between the stator winding of the motor and the grounding wire due to the fluctuation of common mode voltage associated with switching of the inverter[5,7]. In addition, the frequency band of this common mode noise is several MHz or less, and the maximum 1 MHz band is mainly shown to be predominant[7].

In recent years, the adoption of shielded cables for wiring between the servo drive and the motor in a low voltage inverter is becoming the mainstream. Since the shielded cable generates high stray capacitance between the motor power line and the external shield (grounding wire), it is known that high-frequency leakage current becomes high. Generally, when a servo drive system is adopted for robots in production sites, there is a tendency that the number of axes for the servo drive and motor and the cable length increase. Therefore, it is important to evaluate the influence of high-frequency leakage current on the system and the other equipment when the number of axes and the length of shielded cable increase.

The application of shielded cables to low voltage inverters is studied from the viewpoint of common mode noise[8]. On the other hand, the models that can evaluate the influence of high-frequency leakage current of shielded cables on the system (= conducted emission) and the tendency of noise increase due to the increase in the number of axes and the length of the cable are not shown.

In this paper, the technique for analyzing conducted noise of an AC power supply system will be studied for the purpose of shortening the development period for servo drive systems. In particular, in frequency bands up to 1.5 MHz, we will show the analysis technique capable of evaluating the influence of high-frequency leakage current from shielded cables on the system and the other equipment that is an issue common to servo drive systems. The tendency for changes in conducted emission when changing the length and the number of axes of shielded cables was reproduced by this technique to an existing servo drive AC power supply system.

2. Technique for analyzing conducted noise

2.1 Configuration of AC-powered servo drive system

Fig. 2 shows a circuit diagram of an AC-powered servo drive system.

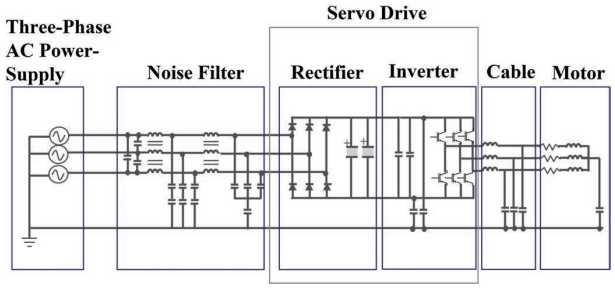

Fig. 2 Circuit diagram of an AC-powered servo drive system

Fig. 2 shows a noise filter for preventing the outflow of conducted noise to the three-phase AC power supply side (system), and AC input is converted to DC by the rectifier circuit of the next stage. Then, DC is converted to three-phase PWM waveforms by switching of the inverter circuit and is supplied to the motor (load) through a power cable.

2.2 Simulation model

Analysis model for conducted noise of an AC-powered servo drive system is shown in Fig. 3. Furthermore, PSIM (Altair Co.) is used as the circuit simulator.

Table 1 shows the main simulation conditions.

Table 1 Main simulation conditions

Item	Parameter
Power supply input	3-phase, 240 V AC, 50 Hz
Output power	200 W
Noise filter	FSB-30-254-HU (Cosel Co.)
Rectifier circuit	Diode rectification
Smoothing circuit	Electrolytic capacitor
Carrier frequency	8 kHz
Power cable	Shielded cable

Conducted emission is evaluated by simulating this model. Models of conducted emission generated by an inverter are so far reported several times[5,6]. The basic configuration of the model in this paper is based on the literature, and only an outline will be described here.

In conducted emission, the LISN (artificial mains network) is connected between the AC power supply and the servo drive, and the noise voltage of the output of the terminal for conducted emission measurement through the high pass filter of the LISN is measured. In this model, the LISN is modeled as an equivalent circuit. Fig. 4 shows the equivalent circuit model of the LISN.

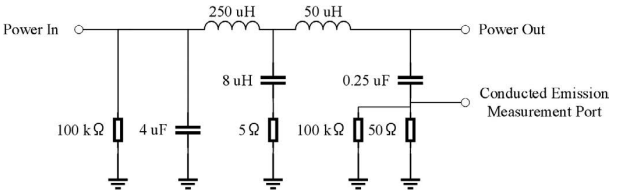

Fig. 4 Equivalent circuit model of the LISN (one axis)

Since the conducted emission is evaluated in the frequency band of 150 kHz–30 MHz, equivalent circuit models of passive components and basic patterns are required to reproduce the impedance characteristics in that band. Fig. 5 shows equivalent circuit models of passive components.

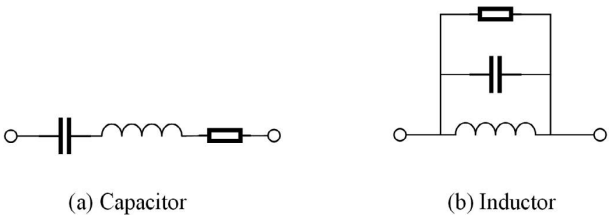

Fig. 5 Equivalent circuit models of passive components

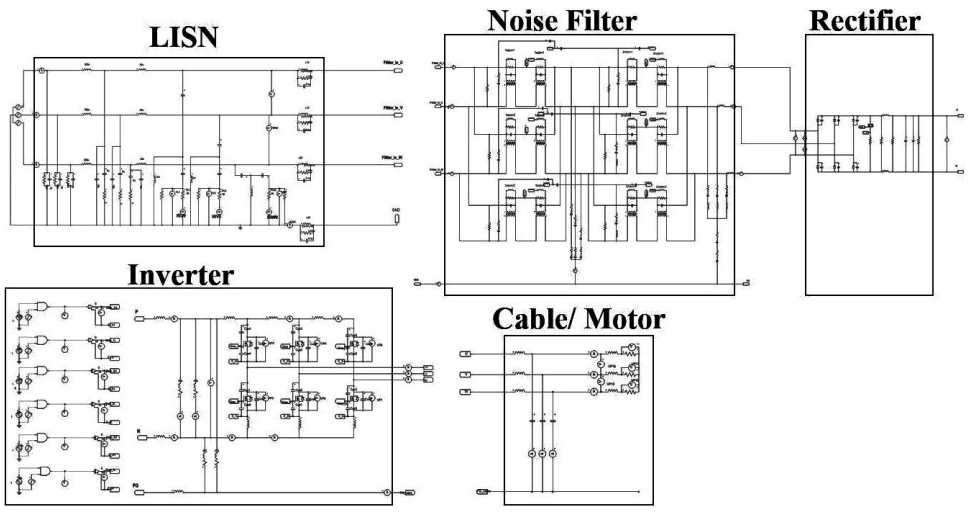

Fig. 3 Simulation model for conducted noise

The circuit constant of equivalent circuit models can be calculated from the impedance frequency characteristics of passive components measured by a network analyzer. In addition, an equivalent circuit model of the substrate wiring can be calculated by simplified calculation from wiring length or electromagnetic field simulation.

3. Modeling of high-frequency leakage current of shielded cable

3.1 Policy of modeling

The main factor in the conducted noise generated in an inverter circuit of the servo drive is common mode noise by the high-frequency leakage current flowing through the stray capacitance between the mechanical parts, such as the motor winding and cable connected to the power semiconductor device of the inverter and grounding wire. In particular, when the cable is shielded, a high stray capacitance of several 10 nH order is generated between the wiring and the shield connected to the grounding wire, and it becomes the main propagation path. This is the value larger than the stray capacitance between the motor winding and the grounding wire by one digit. Since the stray capacitance of the shielded cable is proportional to the cable length, it is considered that the stray capacitance becomes higher as the number of axes of the servo drive and motor and the cable length increase. From the above, we decide on the policy of modeling is the reproduction of the increase/decrease of common mode noise to the changes in the length of the shielded cable and the number of axes and the frequency characteristics.

Common mode noise due to high frequency leakage current is dominant up to 1 MHz band[7]. Therefore, we take the maximum 1.5 MHz as the object of the evaluation in this study. A shielded cable is generally modeled in the distribution constant circuit. Whether we should take the cable model in the distribution constant circuit or the concentration constant circuit depends on the relationship between the frequency and the cable length, and its boundary is unclear. It is said that the frequency in which the cable length is 1/4 of the wavelength is that of the upper limit that can be deemed to be the concentration constant from the rule of thumb. Since the maximum cable length used in a general servo drive system is 50 m, we decided that the upper limit of cable length is 50 m in this study. Since this corresponds to the 1/4 wavelength of 1.5 MHz, we assume that cable can be modeled in a concentration constant circuit in this study. If the cable model can be represented by the concentration constant circuit, the prospect of noise analysis will be improved, and it will be especially useful in the analysis of noise propagation path.

3.2 Switching action

High-frequency leakage current flowing to a grounding wire through stray capacitance between the shield cable wiring and the shield is caused by common mode voltage fluctuations associated with the switching of the inverter. Therefore, at the switching condition in which the common mode voltage fluctuation is the maximum, the high-frequency leakage current becomes the maximum. In the conducted noise simulation model, the switching waveform of the inverter was decided to be that for which the common mode voltage fluctuation becomes the maximum.

Common mode voltage associated with switching of the inverter is expressed by Eq. (1).

$$v_{CM} = \frac{v_u + v_v + v_w}{3} \tag{1}$$

v_u, v_v, v_w: Voltage of each phase of inverter

v_{CM}: Common mode voltage

The amplitude of common mode voltage v_{CM} becomes the maximum during servo-lock operation, and we will promote our discussion of conducted emission at this operation. Figs. 6 and 7 show the inverter circuit and servo-lock operation of inverter, respectively.

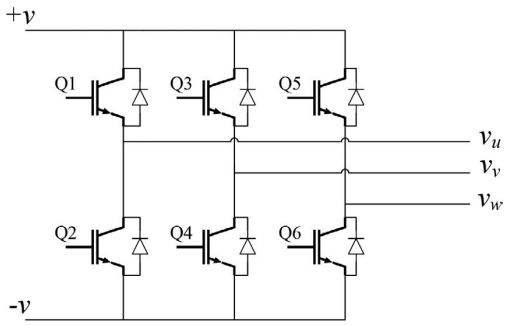

Fig. 6 Inverter Circuit

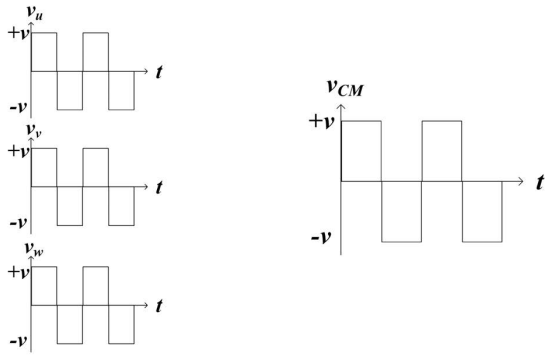

(a) Inverter Phase Voltage (b) Common Mode Voltage

Fig. 7 Servo-lock operation of inverter

3.3 Reproduction of noise increase/decrease to cable length and number of axes

Theoretical studies regarding conducted noise generated when simultaneously operating multiple inverters connected to the same power supply in parallel have been so far performed[9,10]. The configuration where multiple inverters are connected to the same power supply in parallel is equivalent to that of the system with servo drives and motors having multiple axes, and the stray capacitance of a shielded cable increases in proportion to the number of inverters installed in parallel (number of axes). On the other hand, theoretical studies concerning models not including noise filters are performed in every report, and the theoretical formula for conducted emission to the number of axes when a noise filter is included is not shown. Therefore, this paper derives the theoretical formula for conducted emission when a noise filter is included, and clarifies the relational expression between the cable length and the number of axes and the conducted emission.

Fig. 8 shows common mode equivalent circuit of an AC-powered servo drive system shown in Fig. 2.

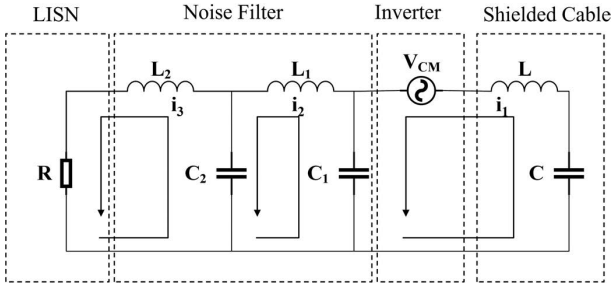

Fig. 8 Common mode equivalent circuit

Fig. 8 shows common mode equivalent circuit shown in the literature[9] added with a noise filter. For an actual common mode equivalent circuit, although the simulation of parasitic impedance, such as wiring and device is required, only the main common mode components were considered in order to simplify the theoretical analysis. Since the influence of parasitic impedance is small in the low-frequency band (about 150 kHz–300 kHz) of conducted emission, it is considered that the equivalent circuit shown in Fig. 8 can be applied. On the other hand, since noise amplification due to resonance arises as a problem in the higher frequency band, analysis that includes the parasitic impedance of wiring and device is required.

Where, v_{CM} represents common mode voltage, and i_1-i_3 is the common mode currents flowing in each part. Two-stage LC filters are adopted as noise filters, L_1 and L_2 represent common mode inductance, and C_1 and C_2 are the capacitor capacitance. Shielded cable is decided to have fixed cable length, L represents the inductance of the shielded cable wiring, and C is the stray capacitance between the shielded cable wiring and the shield. Making R represent the resistance for measurement of conducted emission of LISN, conducted emission v is expressed by Eq. (2).

$$v = Ri_3 \tag{2}$$

Therefore, if i_3 is obtained, the theoretical formula for conducted emission can be derived. The closed-circuit equation of i_1-i_3 of the common mode equivalent circuit shown in Fig. 4 is expressed by Eq. (3).

$$\begin{bmatrix} j\omega_n L + \frac{1}{j\omega_n C} + \frac{1}{j\omega_n C_1} & -\frac{1}{j\omega_n C_1} & 0 \\ -\frac{1}{j\omega_n C_1} & j\omega_n L_1 + \frac{1}{j\omega_n C_1} + \frac{1}{j\omega_n C_2} & -\frac{1}{j\omega_n C_2} \\ 0 & -\frac{1}{j\omega_n C_2} & R + j\omega_n L_2 + \frac{1}{j\omega_n C_2} \end{bmatrix} \begin{bmatrix} i_1 \\ i_2 \\ i_3 \end{bmatrix} = \begin{bmatrix} V_{Cn} \\ 0 \\ 0 \end{bmatrix} \tag{3}$$

V_{Cn} in Eq. (3) is the effective value of harmonics that takes the switching frequency as the basic frequency when common mode voltage v_{CM} is represented by the Fourier series. Here, n represents the degree of harmonics and ω_n the angular frequency of n-degree harmonics. In Eq. (3), when assuming a circuit constant of noise filter $L_1 = L_2 = 7$ mH, $C_1 = 0.11$ μF and $C_2 = 0.05$ μF, then it becomes $1/j\omega C_1 = 9.6$ Ω and $1/j\omega C_2 = 21$ Ω for $\omega L_1 = \omega L_2 = 1050$ Ω at $f = 150$ kHz. At this time, since $\omega L_1 \gg 1/j\omega C_1$ and $\omega L_2 \gg 1/j\omega C_2$ make $i_1 \gg i_2$ and $i_2 \gg i_3$, Eq. (3) can be approximated by Eq. (4).

$$\begin{bmatrix} j\omega_n L + \frac{1}{j\omega_n C} + \frac{1}{j\omega_n C_1} & 0 & 0 \\ -\frac{1}{j\omega_n C_1} & j\omega_n L_1 + \frac{1}{j\omega_n C_2} & 0 \\ 0 & -\frac{1}{j\omega_n C_2} & R + j\omega_n L_2 \end{bmatrix} \begin{bmatrix} i_1 \\ i_2 \\ i_3 \end{bmatrix} = \begin{bmatrix} V_{Cn} \\ 0 \\ 0 \end{bmatrix} \tag{4}$$

If Eq. (4) is solved for i_3, conducted emission is obtained from Eq. (2). Conducted emission V_n of n-order harmonics is expressed as Eq. (5).

$$V_n = \frac{C}{\left(C_1 + C - \omega_n^2 LCC_1\right)} \frac{1}{\left(\omega_n^2 C_1 C_2 - 1\right)} \frac{1}{\sqrt{1 + \left(\frac{\omega_n L_2}{R}\right)^2}} V_{Cn} \tag{5}$$

In Eq. (5), the cable length and the number of axes affect only the first term of the right side. Here, the cable length of the shielded cable is assumed to be l, the number of axes N, stray

capacitance per unit length C_s, and wiring inductance per unit length L_s. Here, if the operation condition of all axes connected in parallel and the cable length are assumed to be the same, C and L in Eq. (5) can be replaced by NC_sl and L_sl/N[9]. From the first term of the right side in Eq. (5), conducted emission is proportional to V_n (l, N) expressed by Eq. (6).

$$V_n(l,N)=\frac{NC_sl}{C_1+NC_sl-\omega_n{}^2C_1L_sC_sl^2} \tag{6}$$

From Eq. (6), the change in the conducted emission when the cable length changes from l_1 to l_2 in the servo drive system of one axis is expressed as Eq. (7).

$$\frac{V_n(l_2,1)}{V_n(l_1,1)}=\frac{l_2}{l_1}\frac{C_1+C_sl_1-\omega_n{}^2C_1L_sC_sl_1^2}{C_1+C_sl_2-\omega_n{}^2C_1L_sC_sl_2^2} \tag{7}$$

From Eq. (6), the change amount of conducted emission when the number of axes of the servo drive system changes from 1 to N is expressed as Eq. (8).

$$\frac{V_n(l,N)}{V_n(l,1)}=N\frac{C_1+C_sl-\omega_n{}^2C_1L_sC_sl^2}{C_1+NC_sl-\omega_n{}^2C_1L_sC_sl^2} \tag{8}$$

If the right sides of Eqs. (7) and (8) are focused on, the length of the shielded cable and the parameter of the number of axes are also included in the second term of the denominator of the right side. From this, it is found that when stray capacitance becomes large to the extent that it is not negligible to capacitor capacitance C_1 of the noise filter, conducted emission is not proportional to the cable length and the number of axes.

Then, the change in the conducted emission to the cable length and the number of axes of the shielded cable in the conducted noise simulation is compared to the theoretical formula. Fig. 9 shows shielded cable and motor model in the conducted noise simulation.

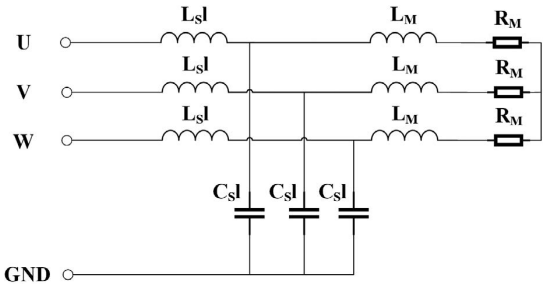

Fig. 9 Shielded cable and motor model

In Fig. 9, L_M and R_M represent the winding inductance and winding resistance of the motor, respectively. In this study, since the high-frequency leakage current from the shielded cable is focused on, the stray capacitance between the motor and the grounding wire is not considered.

Figs. 10 and 11 show the results of the comparison between the theoretical value and the simulation value of the model shown in Fig. 3 for conducted emission (152 kHz) when the cable length and the number of axes are changed, respectively.

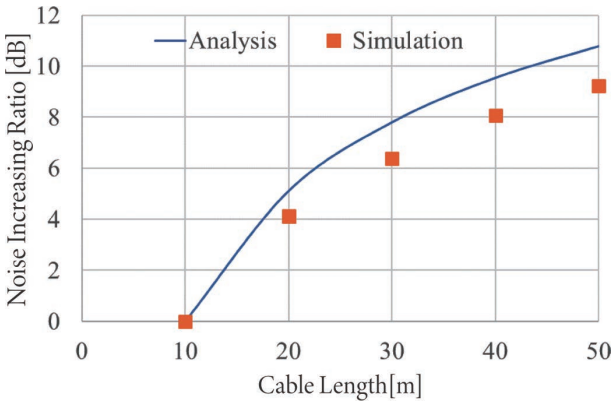

Fig. 10 Change of conducted emission to cable length

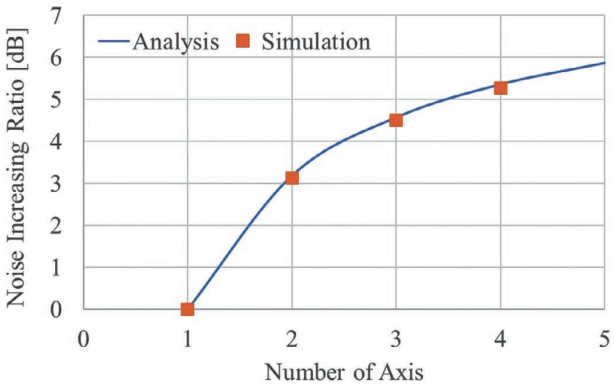

Fig. 11 Change of conducted emission to number of axes

Here, 152 kHz corresponds to 19-order harmonics of common mode voltage, and the minimum odd degree in the frequency band targeted by conducted emission. Fig. 10 shows the theoretical values and the simulation values of the increasing ratio of conducted emission when changing the cable length on the basis of the cable length of 10 m in a uniaxial servo drive system. Fig. 11 shows the theoretical and simulation values of the increasing ratio of conducted emission when changing the number of axes of servo drive to be connected to noise filter from one by fixing cable length to 50 m. From Figs. 10 and 11, it can be said that the increasing ratio of conducted emission to the cable length and the number of axes is not proportional to both theoretical and simulation values, and the conducted noise simulation can reproduce the noise increase/decrease tendency. In addition, from Fig. 11, it is found that the theoretical and simulation values of the increasing ratio of conducted emission to the number of axes coincide well. On the other hand, the increasing ratio of conducted emission to cable

length when reference cable length in Fig. 10 is assumed to be 10 m has errors between the theoretical and simulation values. This is considered because only main common mode components were taken into consideration in the theoretical formula, but parasitic components of wiring board and device were also taken into consideration in simulation values.

From these results, it is found that the analysis, including parasitic impedance of the device and wiring board, is required in order to predict the change in the conducted emission for cable length more accurately.

3.4 Reproduction of frequency characteristics for cable length

It is reported that the resonance of the common mode is generated by the parasitic impedance of the cable when the shielded cable is applied to output wiring of an inverter[7]. Since the resonance by parasitic impedance of the cable amplifies high-frequency leakage current at a particular frequency (resonance frequency), the reproduction of its frequency characteristics is important to evaluate the influence of the high-frequency leakage current on the system and other equipment. Fig. 12 shows the common mode equivalent circuit for analyzing common mode resonance by parasitic impedance of the cable.

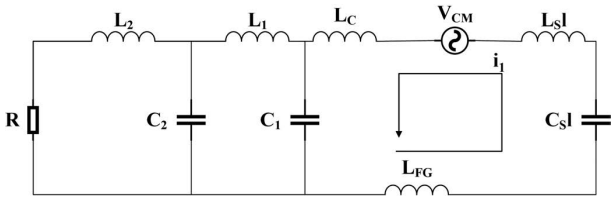

Fig. 12 Common mode equivalent circuit used for resonance analysis

Fig. 12 is the common mode equivalent circuit in Fig. 8 added with L_C and L_{FG}. In Fig. 12, L_C represents inductance of the substrate wiring and other wirings, and L_{FG} inductance of the grounding wire. In addition, the length of the shielded cable is assumed to be l, stray capacitance per unit length C_s, and wiring inductance per unit length L_s. Common mode resonance by parasitic impedance of the cable is LC series resonance in the loop of common mode current i_1 in Fig. 12. Therefore, the theoretical formula of resonance frequency f_r is approximated by Eq. (9).

$$f_r = \frac{1}{2\pi\sqrt{\dfrac{C_1 C_s l}{C_1 + C_s l}\left(L_s l + L_{FG} + L_c\right)}} \tag{9}$$

The resonance frequency means the peak value in the frequency characteristic of noise. In Eq. (9), C_1, C_s, L_s, and l are design values and known parameters. In addition, L_C can be calculated by simplified calculation from the substrate wiring and other wirings configuration. Therefore, L_{FG} becomes an unknown parameter. L_{FG} becomes the sum of inductances of the shield of the shielded cable and grounding wire. Here, wiring between the noise filter and the servo drive is predominant in the grounding wire, and inductance is known. Although inductance per unit length of the shield is unknown, it was approximated as 1/2 of the wiring inductance per unit length from the shielded cable. Eq. (10) is an approximate expression of L_{FG}.

$$L_{FG} = L_g + \frac{L_s l}{2} \tag{10}$$

L_g: Wiring inductance of grounding wire

Fig. 13 shows the results of a comparison between the resonance frequency generated in conducted emission when changing the cable length in a conducted noise simulation in Fig. 3 and the theoretical formula.

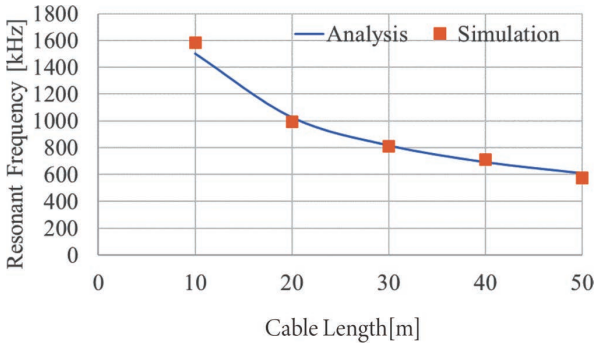

Fig. 13 Change of resonance frequency to cable length

From Fig. 13, it is found that the resonance frequency of the simulation coincides with theoretical value. If the resonance frequency can be evaluated by conducted noise simulation, it is effective for the analysis of the noise mechanism and helpful for the study of noise suppression.

4. Evaluation results of analysis technique

4.1 Evaluation results of increase/decrease of noise to cable length

Evaluation of the validation of the conducted noise simulation was performed by comparing the measurement results of the conducted emission of an AC-powered servo drive system. Table 2 shows the main parameters of an AC-powered servo drive system to be evaluated.

Table 2 Main parameters to be evaluated

Item	Parameter
Power supply input	3-phase, 240 V AC, 50 Hz
Output power	100 W
Noise filter	FSB-30-254-HU (Cosel Co.)
Rectifier circuit	Diode rectification
Smoothing circuit	Electrolytic capacitor
Carrier frequency	16 kHz
Power cable	Shielded cable C: 460 pF/m L: 21 nH/m

In Table 2, capacitance C and inductance L per unit length of shielded cable are the measured values of the manufacturer of the cable used in the experiments. Fig. 14 shows the measurement results of conducted emission when changing the cable length of an AC-powered servo drive system with one axis.

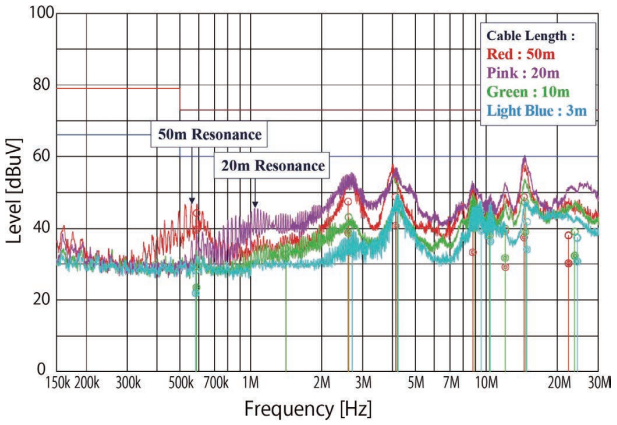

Fig. 14 Measurement results of conducted emission (one axis)

In this study, in order to evaluate the influence of high-frequency leakage current from shielded cable, cable lengths of 10, 20, and 50 m in Fig. 14 where stray capacitance of the shielded cable is considered to be predominant were evaluated. Fig. 15 shows the results of the comparison between the measured and simulation values concerning conducted emission (176 kHz) to cable length on the basis of a cable length of 10 m.

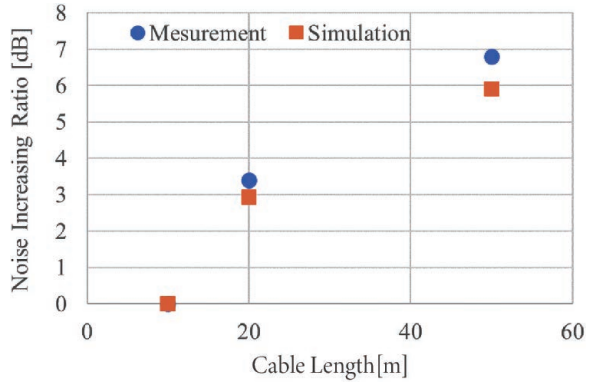

Fig. 15 Change of conducted emission to cable length

From Fig. 15, it is found that the error in the increasing ratio of conducted emission to cable length between the measured and simulation values is ≤ 1 dB and show good coincidence. This result can say that conducted noise simulation successfully reproduced the noise increase/decrease depending on cable length.

4.2 Evaluation results of noise increase/decrease to number of cable axes

Then, the comparison of the measured and simulation values when changing the number of axes of a servo drive system connected to a noise filter in parallel is shown. Fig. 16 shows the measurement results of conducted emission of AC-powered servo drive systems of one axis and three axes.

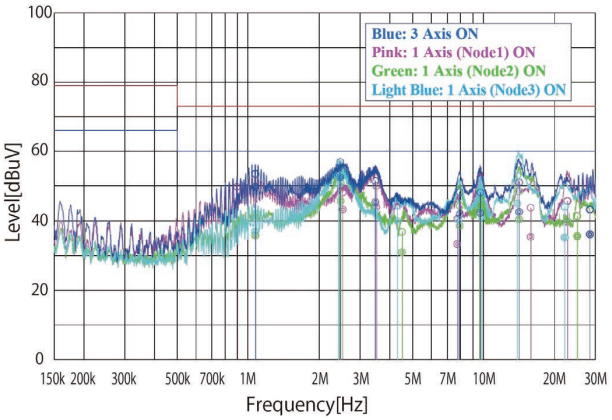

Fig. 16 Change of conducted emission to number of axes

Fig. 16 shows the measured values of conducted emission when operating a servo drive with three axes, one axis by one axis fixing the cable length at 20 m, and when operating the drive with three axes simultaneously. Fig. 16 shows the increasing ratio of conducted emission (176 kHz) of three axes to one axis is 7.3 dB. To this, since simulation result is 6.6 dB, the measured and simulation values can be said to coincide well. This result can say that the conducted noise simulation successfully reproduced the noise increase/decrease depending on the number of axes.

4.3 Evaluation results of frequency characteristic to cable length

Fig. 17 shows the results of the comparison between the measured values and the simulation values in conducted emission (one axis) in Fig. 14 concerning the resonance frequency generated in conducted emission when changing the cable length.

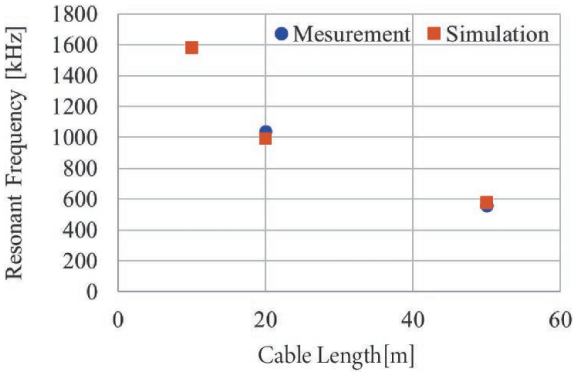

Fig. 17 Change of resonance frequency for cable length

Since no clear resonance peak in a cable length of 10 m was recognized in the measurement results, the results of the measured values only in cable lengths of 20 m and 50 m are shown. From Fig. 17, it is found that the resonance frequency of the simulation coincides with the measured value. This result can say that conducted noise simulation successfully reproduced the frequency characteristic of conducted emission to cable length.

5. Conclusion

This paper studied the analysis technique for conducted noise capable of evaluating the influence of high-frequency leakage current from shielded cable on the system and other equipment for the purpose of shortening the development period for a servo drive. We showed that the increase/decrease of noise and the frequency characteristic to the length of shielded cable and the number of axes can be reproduced by conducted noise simulations by accurately modeling the parasitic components of the substrate wiring and noise filter and the impedance of the grounding wire. As a result, the change tendency of conducted emission when changing the cable length and the number of axes of shielded cable was reproduced for the existing AC-powered servo drive system. We consider that this technology can measure for noise and can reflect in the design of the upstream process of development and can contribute to shortening of the development period for servo drive products.

Hereafter, we will verify the effect of conducted noise analysis techniques by applying this technology to a DC-powered multiaxial servo drive system and extracting and verifying the noise issue caused by high-frequency leakage current from shielded cable in advance.

References

1) Ministry of Environment, “Policy (Menu of Measures) for Industry Sector (Manufacturing Companies),” *Policy for Greenhouse Gas Emission Reduction, etc*, https://www.env.go.jp/earth/ondanka/gel/ghg-guideline/industry/measures/view/86.html, (accessed Jan. 10, 2023).
2) H. Yoshikawa, “Energy Saving System Trend for Harbor Crane with Lithium Ion Battery,” The 2018 International Power Electronics Conference (IPEC-Niigata 2018-ECCA Asia), pp. 219−226, 2018.
3) T. Kiribuchi, T. Zaitsu, M. Doi, Y. Kusaka, and J. Ito, “Analysis of Stability of DC-powered Servo Drive System by Impedance Method,” (in Japanese), *IEEJ D*, vol. 140, no. 3, pp. 184−193, 2020.
4) S. Ogasawara, H. Fujita, and H. Akagi, “Modeling and Theoretical Analysis of High-Frequency Leakage Current Generated by Voltage Type PWM Inverter,” (in Japanese), *IEEJ D*, vol. 115, no. 1, pp. 77−83, 1995.
5) M. Tamate, T. Sasaki, and A. Toba, “Quantitative Estimation Method for Conducted Emission in Inverter by Simulation,” (in Japanese), *IEEJ D*, vol. 128, no. 3, pp. 193−200, 2008.
6) A. Minegishi, K. Sakiyama, and T. Yamada, “Study of Analysis Technique for Common Mode Noise of Inverter Power Supply Circuit,” (in Japanese), *IEICE Tech. Rep.*, vol. 112, no. 100, EMCJ2012−23, pp. 14−16, 2012.
7) S. Hanioka, M. Iezawa, S. Ogasawara, M. Takemoto, and K. Orikawa, “Common Mode Noise Suppression Control of Two-Motor Drive System,” (in Japanese), *IEEJ D*, vol. 141, no. 11, pp. 895−902, 2021.
8) T. Tsuchida, “Study Concerning Application of Shielded Cable to Inverter Output Wiring,” (in Japanese), *IEEJ D*, vol. 132, no. 7, pp. 718−726, 2012.
9) K. Wada, T. Ishizuka, and T. Shimizu, “Conducted Noise of AC Module Type System Interconnection Inverter System and its Suppression Method,” (in Japanese), *IEEJ D*, vol. 125, no. 10, pp. 911−918, 2005.
10) M. Tamate, A. Toba, Y. Matsumoto, K. Wada, and T. Shimizu. “Method for Controlling Carrier Phase Suitable for Reduction of Conducted Emission in System Configured by Multiple Power Conversion Equipment,” (in Japanese), *IEEJ D*, vol. 131, no. 6, pp. 811−819, 2011.

About the Authors

HAMANA Kentaro

Digital Design Center
Technology and Intellectual Property H.Q.
Specialty: Electrical and Electronics Engineering
Affiliated Academic Society: IEICE

TOKUSAKI Hiroyuki

Advanced Technology Development Dept.
Advanced Technology Center
Technology and Intellectual Property H.Q.
Specialty: Electrical Engineering

UEMATSU Takeshi, Ph.D. (Engineering)

Advanced Technology Development Dept.
Advanced Technology Center
Technology and Intellectual Property H.Q.
Specialty: Electrical Engineering
Affiliated Academic Society: IEEJ, IEICE